Indian Journal of Geo Marine Sciences
Vol. 49 (05), May 2020, pp. 889-897

The transient free convection magnetohydrodynamic motion of a nanofluid over a vertical surface under the influence of radiation and heat generation

P S Rao[b], Om Prakash[b,c], S R Mishra[d] & R P Sharma*[,a]

[a]Department of Mechanical Engineering, National Institute of Technology Arunachal Pradesh – 791 112, India

[b]Department of Mathematics & Computing, IIT (ISM), Dhanbad – 826 006, India

[c]Department of Mathematics, JECRC University, Jaipur – 303 905, India

[d]Department of Mathematics, S 'O' A Deemed to be University, Khandagiri, Bhubaneswar, Odisha – 751 030, India

*[E-mail: rpsharma@nitap.ac.in]

Received 30 October 2018; revised 18 June 2018

The main purpose of this article is to study the effect of MHD, internal heat generation, thermal radiation and nanoparticle volume mass on an unsteady free convection motion of a nanofluid over the infinite vertical sheet. Nanofluids involving nanoparticles of silver, aluminum oxide, copper and titanium oxide with a nanoparticle volume concentration range smaller than or equal to 0.04 were taken. The numerical solutions of governing boundary value problems were gained by the Laplace transform algorithm and symbolic computation software MATLAB. The effects of MHD, heat generation, radiation and nanoparticle volume concentration on the velocity, energy and mass descriptions are depicted graphically. The skin friction coefficient, Nusselt number and Sherwood number are also investigated.

[**Keywords**: Free convection, Heat generation, MHD flow, Nanofluid, Radiation]

Introduction

In current years several researchers have studied free convection motion of a viscous incompressible liquid through a vertical sheet due to its broad applications in the nuclear cooling structure model. In nuclear reactors, a reactor is a device employed to initiate and control a sustained nuclear chain reaction. The reactor is made of many parallel vertical plates with heat generation. Liquid cooling and heating participate in pivotal tasks in various industrial and technological processes, especially in nuclear reactors, power generation and transportation, thin-film, solar power collectors and in much more execution. These processes, utilize the established heat transfer fluids, for example, ethylene glycol, oil and water heat transfer capacity due to very low thermal conductivity.

The accumulation of solid nanoparticles to these ordinary liquids enhances thermal conductivity. Thus a base fluid (water, oil, ethylene glycol, etc.) involving solid nanoparticles (for example Al_2O_3, Cu, TiO_2, Ag, etc.) is known as nanofluid[1]. Nanofluids have been proved to be free from problems for example high-pressure drop, erosion, sedimentation, and a smaller particle volume fraction is required to enhance the energy transfer as differentiated to microparticle slurries. Parida and Mishra[2] have studied the heat and mass transfer of magnetohydrodynamic motion of nanofluids under the influence of chemical reaction and magnetic field. Kuznetsov and Nield[3] have analyzed the free convection laminar motion of a nanofluid over a vertical surface under the influence of Brownian flow and thermophoresis. Wakif *et al.*[4] have reported Buongiorno's mathematical model for examining the impacts of a uniform transverse magnetic field and the volumetric fraction of nanoparticles. They have studied various aspects of the contribution of physical parameters on the flow phenomena that enhances the thermal properties. Moreover, they have used an approximate analytical technique to solve the complex nonlinear coupled differential equations. Makinde and Mishra[5] have studied the influence of thermal radiation on the stagnation point laminar motion of inconsistent viscosity water base nanofluid past an extending sheet. The novelty of their work is the study of streamlines for various stream functions. Sithole *et al.*[6] studied the unsteady magnetohydrodynamic Maxwell nanofluid motion

over a reduction sheet under the influence of Brownian motion and thermophoresis, convective and slip boundary situations. Hayat *et al.*[7] analyzed the melting transfer of energy of a stagnation position flow of nano liquid past an expanding surface with thermal radiation and heat source/sink. The effect of melting is to draw the heat from the surface of the fluid in its boundary layer. It also provides a significant reduction in the rate of heat transfer near the surface. In an effort, Stokes[8] has analyzed an unsteady motion over a spontaneously started infinite sheet. The problem considered by Stokes is the primary problem in fluid mechanics and energy transfer and is famous as Stokes's problems. Raptis and Tzivanidis[9] investigated the impacts of the heat source and mass transfer on the Stokes problem for an infinite vertical sheet. Many researchers[10-13] studied that the thermal conductivity of exclusion can enhance by over 25 % with a very small nanoparticle volume concentration. Pak and Cho[14] reported heat transfer in 2 types of nanofluids and reported that with an increase in the volume fraction of suspended solid particles and Reynolds number, the corresponding Nusselt number of the isolated liquid enhances. Wen and Ding[15] have examined natural convective nanofluids connecting titanium oxide particles. Loganathan *et al.*[16] explored the importance of radiation and nanoparticle concentration on an unsteady free convection motion of a nanofluid over an infinite perpendicular sheet. Rohni *et al.*[17] reported the unsteady motion over a continuously shrinking sheet in the presence of wall mass suction in nanofluids. The boundary layer of an unsteady 2-D stagnation-point motion of a nanofluid was investigated by Bachok *et al.*[18]. Sheikholeslami *et al.*[19] have analyzed the impact of radiation on MHD nanofluid motion and the transfer of heat of 2-phase mathematical representation. Further, Sheikholeslami and Ganji[20] have analyzed the nanofluid with a magnetic field. Sheikholeslami and Rashidi[21] have shown the impact of space-dependent magnetic field on natural convection of Fe_3O_4–water nanofluid. Sheikholeslami *et al.*[22] have studied magneto-hydro-dynamic natural convection of Alumina–water nanofluid with radiation. Sheikholeslami *et al.*[23] have shown that the impact of the non-uniform magnetic field on the forced convective transfer of heat of Fe_3O_4-water nanofluid. Khan and Pop[24] have studied that the laminar motion of a water-based nanofluid past an extending sheet. Das *et al.*[25] have studied an unsteady free convective motion over a vertical sheet under the influence of heat and mass fluxes through radiation. Shehzad *et al.*[26] have reported the effect of convection transfer of heat and mass conditions with the magnetohydrodynamic motion of water-based nanofluid. Hayat *et al.*[27] have studied magneto-hydro-dynamic 3-D motion of nanofluid with slip velocity and radiation. Das *et al.*[28] have investigated the transient natural convective in a vertical waterway filled with nanofluids with radiation. Kameswaran *et al.*[29] have analyzed that nanofluids saturated permeable medium under the influence of convection boundary circumstances. Awad *et al.*[30] investigated those dual scattering results in a nanofluid motion in the presence of a non-Darcy permeable media. Rashadi *et al.*[31] investigated the significance of nanofluid saturated non-Darcy porous medium with viscous dissipation on mixed convection under the convective boundary condition.

The key intent of this effort is to examine velocity, the transfer of heat and mass of nanofluids on magnetohydrodynamic, thermal radiation and heat generation impacts on a transient free convection motion of Ag, TiO_2, Al_2O_3, Cu and nanoparticles among water while a base liquid over an infinite perpendicular sheet.

Materials and Methods

Mathematical Model

The present study has examined an unsteady MHD natural convective 2-D motion of an incompressible electrically conducting nanofluid over an impetuously vertical sheet with thermal radiation. The direction of motion is taken along the $x-$axis directed alongside

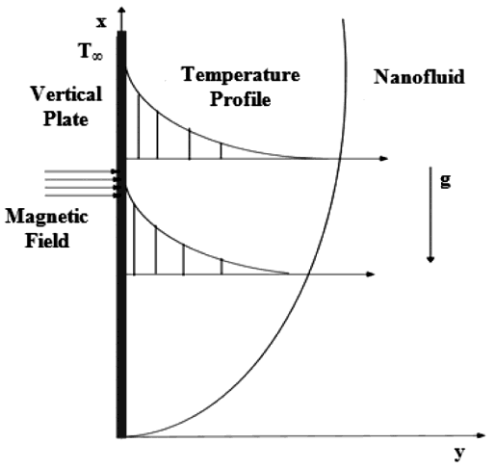

Fig. 1 — Flow Schematic diagram

the vertical sheet in the upward direction, and the $y-$axis is assumed normal to it (Fig. 1).

Initially, at $t' \le 0,$ the sheet and nanofluid are taken at a similar temperature. At $t' \le 0,$ the sheet is in the position of rest, at $t' > 0,$ the plate initiates to move in the vertical direction having a constant velocity u_0. we consider the viscous dissipation effect to be negligible, and the fluid has a volumetric rate of heat generation Q_0. The temperature T_ω of the surface is taken as a stable and is superior to the temperature of the ambient nanofluid T_∞. In this study, we have taken water-based nanofluids, each involving four different kinds of nanoparticles i.e. copper, silver, aluminum oxide, and titanium oxide.

The basic unsteady momentum, energy and concentration equations based on the mathematical representation for nanofluids presented by Tiwari & Das[32] are

$$\frac{\partial u}{\partial t'} = \frac{\mu_{nf}}{\rho_{nf}}\frac{\partial^2 u}{\partial y^2} + \frac{1}{\rho_{nf}}(\rho\beta)_{nf}\, g(T-T_\infty) + \frac{1}{\rho_{nf}}(\rho\beta^*)_{nf}\, g(C-C_\infty) - \frac{\sigma {B_0}^2}{\rho_{nf}}u - \frac{\nu_{nf}}{K}u, \quad \ldots (1)$$

$$\frac{\partial T}{\partial t'} = \frac{\kappa_{nf}}{(\rho Cp)_{nf}}\frac{\partial^2 T}{\partial y^2} - \frac{Q_0}{(\rho Cp)_{nf}}(T-T_\infty) + \frac{16\sigma^*}{3\kappa^*(\rho Cp)_{nf}}\frac{\partial}{\partial y}\left(T_\infty^3\frac{\partial T}{\partial y}\right) \quad \ldots (2)$$

$$\frac{\partial C}{\partial t'} = D_m\frac{\partial^2 C}{\partial y^2} - k_c(C-C_\infty) \quad \ldots (3)$$

with boundary conditions

$$\left.\begin{array}{l} t' \le 0, u = 0,\ T = T_\infty,\ \ C = C_\infty \ for\, all\, y \\ t' > 0,\ u = u_0,\ T = T_w,\ C = C_w \, at\, y = 0 \\ u \to 0,\ T \to T_\infty,\ C \to C_\infty \ as\, y \to \infty \end{array}\right\} \quad \ldots (4)$$

Employing the Rosseland estimation for thermal radiation by Brewster[34], the radiation energy flux is simplified to

$$q_r = -\frac{4\sigma^*}{3k^*}\frac{\partial T^4}{\partial y}, \quad \ldots (5)$$

and

$$\frac{\partial q_r}{\partial y} = -\frac{16\sigma^* T_\infty^3}{3k^*}\frac{\partial^2 T}{\partial y^2} \quad \ldots (6)$$

It is supposed that there is temperature variation in the motion, the expression T^4 in Taylor's series about T_∞ and omitting high-order expressions[33-36], thus

$$T^4 \approx 4T_\infty^3 T - 3T_\infty^4 \quad \ldots (7)$$

The expressions of density ρ_{nf}, thermal expression coefficient $(\rho\beta)_{nf}$, and heat capacitance $(\rho Cp)_{nf}$ are expressed as

$$\left.\begin{array}{c} \rho_{nf} = \rho_s\phi + \rho_f(1-\phi),\quad (\rho\beta)_{nf} = (1-\phi)(\rho\beta)_f + \phi(\rho\beta)_s, \\ (\rho\beta^*)_{nf} = (1-\phi)(\rho\beta^*)_f + \phi(\rho\beta^*)_s, \\ (\rho Cp)_{nf} = \phi(\rho Cp)_s + (1-\phi)(\rho Cp)_f, \end{array}\right\} \quad \ldots (8)$$

The efficient thermal conductivity of the nanofluid computed with the help of the Maxwell-Garnett model in the following form is

$$\frac{k_{nf}}{k_f} = \frac{k_s + 2k_f - 2\phi(k_f - k_s)}{k_s + 2k_f + \phi(k_f - k_s)} \quad \ldots (9)$$

The above thermal conductivity model is used only when nanoparticles are spherical. Brinkman has given the effective viscosity of the nanofluids follows:

$$\mu_{nf} = \mu_f(1-\phi)^{-2.5} \quad \ldots (10)$$

Table 1 contains the thermophysical properties of the nanofluids. Now let us introduce the subsequent dimensionless variables:

$$U = \frac{u}{u_0}, t = \frac{t'u_0^2}{\nu_f}, Y = \frac{yu_0}{\nu_f}, \theta = \frac{T-T_\infty}{T_w - T_\infty}, \xi = \frac{C-C_\infty}{C_w - C_\infty}, Ra = \frac{\kappa_f k^*}{4\sigma^* T_\infty^3},$$

$$Q = \frac{Q_0\nu_f}{u_0^2(\rho C_p)_f}, K_{ch} = \frac{k_c\nu_f}{u_0^2},$$

$$Gm = \frac{g\beta^*(C_w - C_\infty)\nu_f}{u_0^3}, \Pr = \frac{\nu_f}{\alpha_f}, Sc = \frac{\nu_f}{D_m}, Gr = \frac{g\beta(T_w - T_\infty)\nu_f}{u_0^3},$$

$$M = \frac{\sigma B_0^2\nu_f}{\rho_f u_0^2}, Kp = \frac{\nu_{nf}\nu_f}{Ku_0^2}, \quad \ldots (11)$$

Now the dimensionless governing partial differential equations (1), (2) and (3) with boundary conditions (4) reduce in the following form

$$\frac{\partial U}{\partial t} = \beta_1\frac{\partial^2 U}{\partial Y^2} + \beta_2\theta + \beta_3\xi - \beta_4 U \quad \ldots (12)$$

Table. 1 — Thermophysical characteristic of nanoparticle & pure water

Nanofluid Component	Pure water (H_2O)	Silver (Ag)	Alumina (Al_2O_3)	Copper (Cu)	Titanium oxide (TiO_2)
$\rho[kgm^3]$	997.1	10500.0	3970.0	8933.0	4250.0
$C_P\left(\frac{J}{kg.K}\right)$	4179	235.0	765.0	385.0	686.2
$\kappa\left(\frac{W}{(m.K)}\right)$	0.613	429	40	401	8.9528
$\beta\times10^5\left(K^{-1}\right)$	21	1.89	0.85	1.67	0.9

$$\frac{\partial\theta}{\partial t}=\beta_5\frac{\partial^2\theta}{\partial Y^2}-\beta_6\theta \quad \ldots (13)$$

And $$\frac{\partial\xi}{\partial t}=\frac{1}{Sc}\frac{\partial^2\xi}{\partial Y^2}-K_{ch}\xi \quad \ldots (14)$$

and the transformed boundary conditions are:

$$\left.\begin{aligned} &t\le 0, U=0, \theta=0,\ \xi=0 \ for\ all\ Y,\\ &t>0, U=1, \theta=1,\ \xi=1 \ for\ Y=0,\\ &U\to 0, \theta\to 0,\ \xi\to 0 \ \ for Y\to\infty, \end{aligned}\right\} \quad \ldots (15)$$

Where,

$$\beta_1=\frac{(1-\phi)^{-2.5}}{\left(1-\phi+\phi.\frac{\rho_s}{\rho_f}\right)},\beta_2=\frac{\left[1-\phi+\phi.\frac{(\rho\beta)_s}{(\rho\beta)_f}\right]}{\left[1-\phi+\phi.\frac{\rho_s}{\rho_f}\right]}Gr,\beta_3=\frac{\left[1-\phi+\phi.\frac{(\rho\beta^*)_s}{(\rho\beta^*)_f}\right]}{\left[1-\phi+\phi.\frac{\rho_s}{\rho_f}\right]}$$

$$Gm,\beta_6=\frac{Q}{\left[1-\phi+\phi.\frac{(\rho C_p)_s}{(\rho C_p)_f}\right]}$$

$$\beta_5=\frac{1}{\left[1-\phi+\phi.\frac{(\rho C_p)_s}{(\rho C_p)_f}\right]}\left(\frac{\kappa_{nf}}{\kappa_f}+\frac{4}{3Ra}\right)\frac{1}{\Pr},$$

$$\beta_4=\frac{M}{\left(1-\phi+\phi.\frac{\rho_s}{\rho_f}\right)}+Kp,$$

Equations (12)-(14) with (15) are explained by applying the LT method. The momentum U, energy θ, and concentration ξ are acquired as

$$U=\frac{1}{2}(G_1+G_2)+\frac{\beta_2\beta_5(\beta_1-\beta_5)}{2Z}[e^{Zt}(H_1+H_2-I_1+I_2)+(B_1+B_2-G_1-G_2)]+\frac{\beta_3(Sc\beta_1-1)}{2Z_1}[e^{Z_1t}(J_1+J_2-K_1-K_2)+(A_1+A_2-G_1-G_2)] \quad \ldots (16)$$

$$\theta=\frac{1}{2}(B_1+B_2) \quad \ldots (17)$$

$$\xi=\frac{1}{2}(A_1+A_2) \quad \ldots (18)$$

Where,

$$A_1=\exp\left(2\eta\sqrt{K_{ch}Sct}\right)erfc\left(\eta\sqrt{Sc}+\sqrt{K_{ch}t}\right),$$

$$A_2=\exp\left(-2\eta\sqrt{K_{ch}Sct}\right)erfc\left(\eta\sqrt{Sc}-\sqrt{K_{ch}t}\right),$$

$$B_1=\exp\left(2\eta\sqrt{\frac{\beta_6 t}{\beta_5}}\right)erfc\left(\frac{\eta}{\sqrt{\beta_5}}+\sqrt{\beta_6 t}\right),$$

$$B_2=\exp\left(-2\eta\sqrt{\frac{\beta_6 t}{\beta_5}}\right)erfc\left(\frac{\eta}{\sqrt{\beta_5}}-\sqrt{\beta_6 t}\right),$$

$$G_1=\exp\left(2\eta\sqrt{\frac{\beta_4 t}{\beta_1}}\right)erfc\left(\frac{\eta}{\sqrt{\beta_1}}+\sqrt{\beta_4 t}\right),$$

$$G_2=\exp\left(-2\eta\sqrt{\frac{\beta_4 t}{\beta_1}}\right)erfc\left(\frac{\eta}{\sqrt{\beta_1}}-\sqrt{\beta_4 t}\right),$$

$$H_1=\exp\left(2\eta\sqrt{\frac{(Z+\beta_4)t}{\beta_1}}\right)erfc\left(\frac{\eta}{\sqrt{\beta_1}}+\sqrt{(Z+\beta_4)t}\right),$$

$$H_2=\exp\left(-2\eta\sqrt{\frac{(Z+\beta_4)t}{\beta_1}}\right)erfc\left(\frac{\eta}{\sqrt{\beta_1}}-\sqrt{(Z+\beta_4)t}\right),$$

$$I_1=\exp\left(2\eta\sqrt{\frac{(Z+\beta_6)t}{\beta_5}}\right)erfc\left(\frac{\eta}{\sqrt{\beta_5}}+\sqrt{(Z+\beta_6)t}\right),$$

$$I_2=\exp\left(-2\eta\sqrt{\frac{(Z+\beta_6)t}{\beta_5}}\right)erfc\left(\frac{\eta}{\sqrt{\beta_5}}-\sqrt{(Z+\beta_6)t}\right),$$

$$J_1 = \exp\left(2\eta\sqrt{\frac{(Z_1+\beta_4)t}{\beta_1}}\right)erfc\left(\frac{\eta}{\sqrt{\beta_1}}+\sqrt{(Z_1+\beta_4)t}\right),$$

$$J_2 = \exp\left(-2\eta\sqrt{\frac{(Z_1+\beta_4)t}{\beta_1}}\right)erfc\left(\frac{\eta}{\sqrt{\beta_1}}-\sqrt{(Z_1+\beta_4)t}\right),$$

$$K_1 = \exp\left(2\eta\sqrt{(Z_1+K_{ch})Sct}\right)erfc\left(\eta\sqrt{Sc}+\sqrt{K_{ch}t}\right),$$

$$K_2 = \exp\left(-2\eta\sqrt{(Z_1+K_{ch})Sct}\right)erfc\left(\eta\sqrt{Sc}-\sqrt{K_{ch}t}\right),$$

$$Z=\frac{\beta_5\beta_4-\beta_6\beta_1}{\beta_1-\beta_5}, Z_1=\frac{\beta_4-K_{ch}Sc\beta_1}{Sc\beta_1-1}, \ \eta=\frac{Y}{2\sqrt{t}}$$

The Nusselt number, skin friction coefficient, and Sherwood number are given by

$$\left.\begin{aligned} Nu &= -\frac{1}{2\sqrt{t}}\left(\frac{\kappa_{nf}}{\kappa_f}+\frac{4}{3Ra}\right)\left(\frac{\partial\theta}{\partial\eta}\right)_{\eta=0} \\ C_f &= \frac{1}{2\sqrt{t}}(1-\varphi)^{-2.5}\left(\frac{\partial U}{\partial\eta}\right)_{\eta=0} \\ Sh &= -\left(\frac{\partial\xi}{\partial\eta}\right)_{\eta=0} \end{aligned}\right\} \quad \ldots (19)$$

Results and Discussion

The PDE (12), (13) and (14) with boundary condition equation (15) are calculated by using the Laplace transform method to obtain the exact result. The numerical simulation is done for the diverse values of variables concerned with the problem. The range of nanoparticle volume concentration is taken in the range $0 \le \phi \le 0.06$. If nanoparticle volume concentration exceeds 8 percent then sedimentation takes place.

In the current investigation, the spherical shape of nanoparticles is considered. We have taken pure water-based nanofluids, copper, titanium oxide aluminum oxide and silver. The value of the Pr of the liquid is assumed to be 6.2 for numerical simulation. The momentum (U), energy (θ), and concentration (ξ) are calculated by the equations (16), (17) and (18) respectively.

The transient velocity U is shown is related to a parameter function η for diverse values of nanoparticle volume concentration ϕ and M in Figure 2 for Copper-water nanofluid. It is noticed that the velocity reduces as the value of nanoparticle volume concentration ϕ and M enhances. Because, increasing the transverse magnetic field of a conductive fluid produces a resistance called Lorentz force, similar to drag force and increasing the value of M tends to increase drag force and reduce fluid velocity and the liquid embellishes extra viscous by enhancing the value of nanoparticle volume friction ϕ which guides to reduce the nanofluids momentum. In Figure 3, the velocity description U of the aluminum oxide water nanofluid as a function of η for distinct values of the time t and Hartmann number M. Figure 3 indicates that the momentum reduces as the value of time t and Hartmann number M enhances. In Figure 4, the velocity description U of the silver water nanofluid is related to a parameter function of η for distinct values of ϕ and Hartmann number M. Figure 4 indicates that the momentum reduces as the value of ϕ and Hartmann number M enhances. Figure 5 shows the velocity profile U is related to a parameter function of η for nanofluid containing different nanoparticles. Figure 5 indicates that the velocity is different for different nanofluid and the velocity of silver-water nanofluid is smaller compared to the other nanofluids. In Figure 6, the momentum distribution U is related to a parameter function η for distinct values of Kp and Gm for different nanoparticles. In Figure 6(a), for silver water nanofluid, we noticed that the momentum reduces as

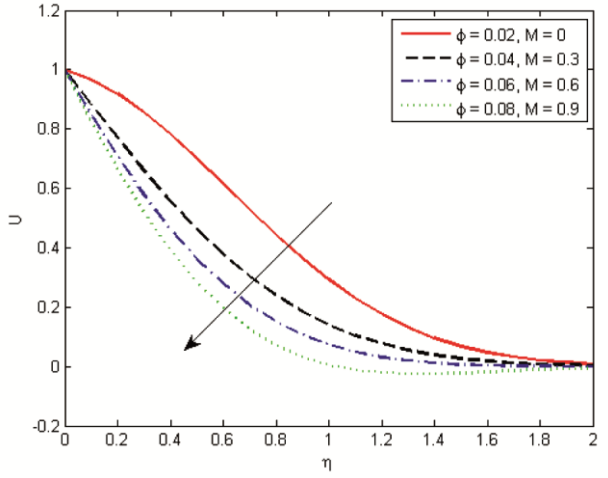

Fig. 2 — Velocity U versus the parameter η for a Copper-water nanofluid at $\Pr = 6.2,\ Gr = 6, Q = 0.4, Sc = 1.5,\ t = 0.2,\ Gm = 3,\ K_{ch} = 0.5, Ra = 1$ and $Kp = 1$ for different values of nanoparticle volume concentration ϕ and M

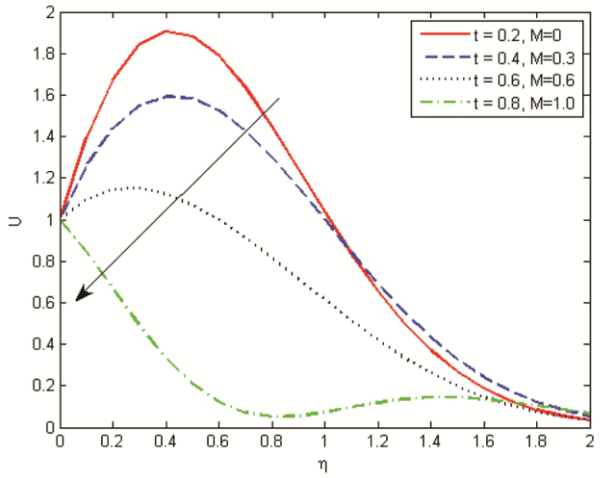

Fig. 3 — Velocity U versus the parameter η for an Aluminum oxide water nanofluid at $\Pr = 6.2, Gr = 6, \ Sc = 1.5, Q = 0.4, K_{ch} = 0.5, \ \phi = 0.06, Gm = 3, \ Ra = 1 \ and \ Kp = 1$ or different values of M and time t

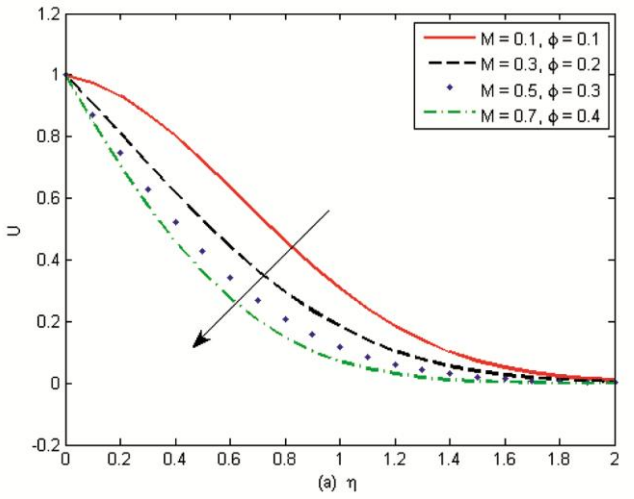

Fig. 4 — Velocity U versus the parameter η for a Silver water nanofluid at $\Pr = 6.2, Gr = 6, Sc = 1.5, \ Q = 0.4, t = 0.2, K_{ch} = 0.5, \ Kp = 1, Gm = 3, \ and \ Ra = 1$ for different values of M, and ϕ .

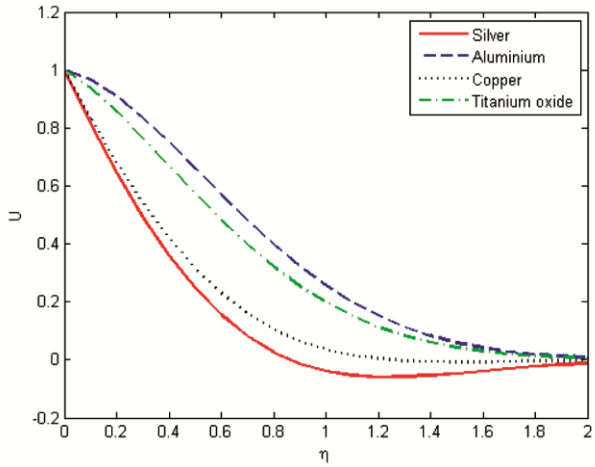

Fig. 5 — Velocity U versus the parameter η at $\Pr = 6.2, Gr = 6, M = 1, Kp = 1, Sc = 1.5, Q = 0.4, \phi = 0.06, K_{ch} = 0.5 \quad Gm = 3, Ra = 1$ and $t = 0.2$ for different nanoparticle.

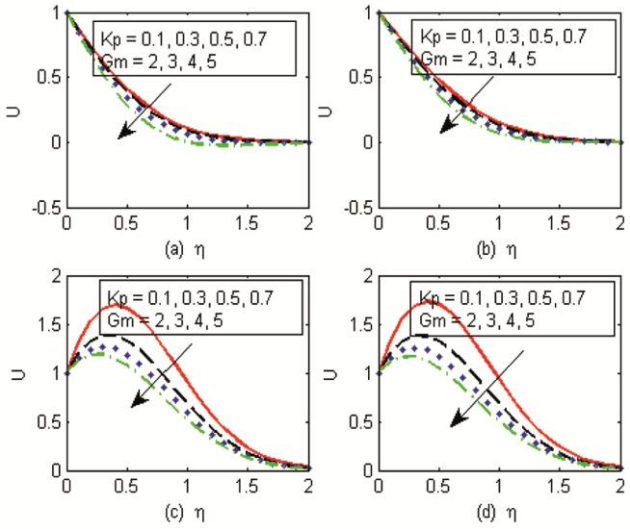

Fig. 6 — Velocity U versus the parameter η at $Gr = 6, \Pr = 6.2, \ Sc = 1.5, Q = 0.4, t = 0.2, \phi = 0.06, \ M = 1, Ra = 1$ and $K_{ch} = 0.5$ for different values of Kp and Gm (a): Silver water nanofluid; (b): Copper water nanofluid; (c): Aluminium oxide-water nanofluid; and (d): Titanium oxide-water nanofluid.

the value of Kp and Gm enhances. In Figure 6(b), for copper water nanofluid, we noticed that the momentum reduces as the value of Kp and Gm enhances. In Figure 6(c) for aluminum oxide-water nanofluid, we noticed that the momentum reduces as the value of Kp and Gm enhances. In Figure 6(d), for titanium oxide-water nanofluid, we noticed that the momentum reduces as the value of Kp and Gm enhances.

In Figure 7, the momentum distribution U is related to a parameter function η for distinct values of chemical reaction K_{ch} for different nanoparticles. In Figure 7(a), for copper water nanofluid, we have seen that the momentum improves as the value of chemical reaction K_{ch} increases. In Figure 7(b), for silver water nanofluid, we have seen that the momentum improves as the value of chemical reaction K_{ch} increases. In Figure 7(c), for aluminum oxide-water nanofluid, we noticed that the momentum enhances as

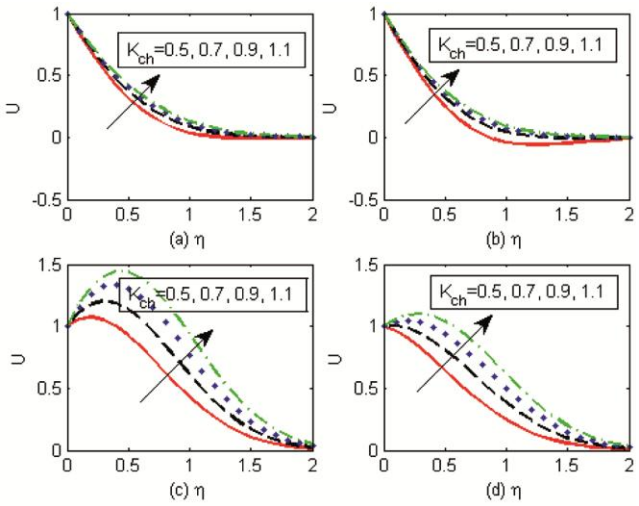

Fig. 7. Velocity U versus the parameter η at $\Pr = 6.2,\ Gr = 6,\ Sc = 1.5, Q = 0.4,\ t = 0.2,\ \phi = 0.6,\ Kp = 1,$ $M = 1, Gm = 3$ *and* $Ra = 1$ for different values of K_{ch} (a): Copper water nanofluid; (b): Silver water nanofluid; (c): Aluminum oxide-water nanofluid; and (d): Titanium oxide-water nanofluid.

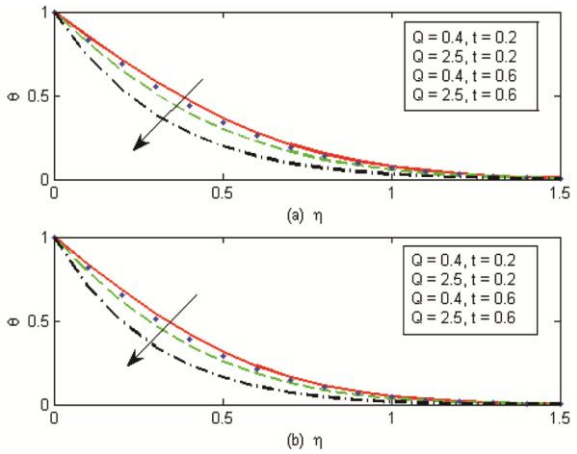

Fig. 8 — Temperature θ versus the parameter η at $\Pr = 6.2,\ \phi = 0.6$ and $Ra = 1$ for diverse values of time t and Q (a): Copper water nanofluid; (b): Titanium oxide-water nanofluid.

the value of chemical reaction K_{ch} increases. In Figure 7(d), for titanium oxide-water nanofluid, we noticed that the momentum improves as the value of K_{ch} enhances.

In Figure 8, The temperature θ is shown is related to a parameter function η for diverse values of Q and t for copper-water nanofluid and titanium oxide - water nanofluid, we observed in Figure 8(a), the temperature reduces as the value of Q and t enhances for copper-water nanofluid and we observed

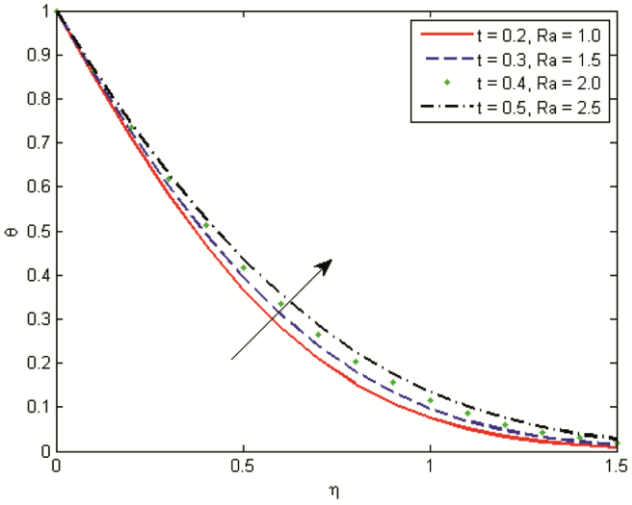

Fig. 9 — Temperature θ versus the parameter η for a Copper water nanofluid at $\Pr = 6.2,\ \phi = 0.04$ *and* $Q = 0.4$ for different values of the time t and *Ra*.

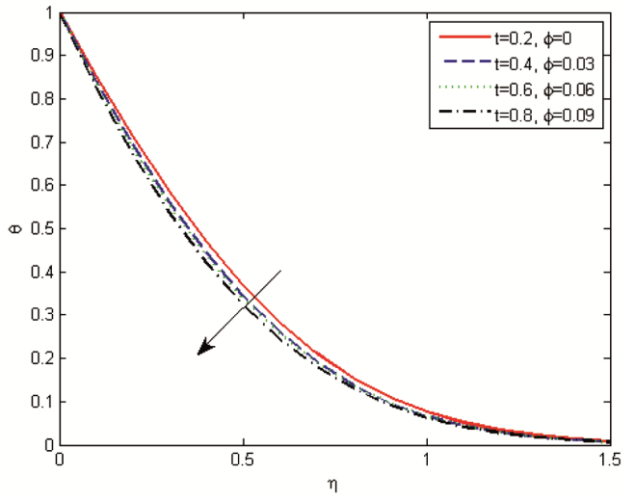

Fig. 10 — Temperature θ versus the parameter η for an Aluminium oxide water nanofluid at $\Pr = 6.2,$ $Q = 0.4$ *and* $Ra = 2$ for different values of nanoparticles volume concentration ϕ and time t.

in Figure 8(b) the temperature reduces as the value of Q and t enhances for titanium oxide-water nanofluid. Because enhance in the fluid temperature causes extra induce motion in the direction of the surface during the thermal buoyancy impact and the higher value of Q the thickness of the thermal boundary film is reduces.

In Figure 9, The temperature θ is depicted is related to a function of the parameter η for distinct values of Ra and time t for copper-water nanofluid. It can be

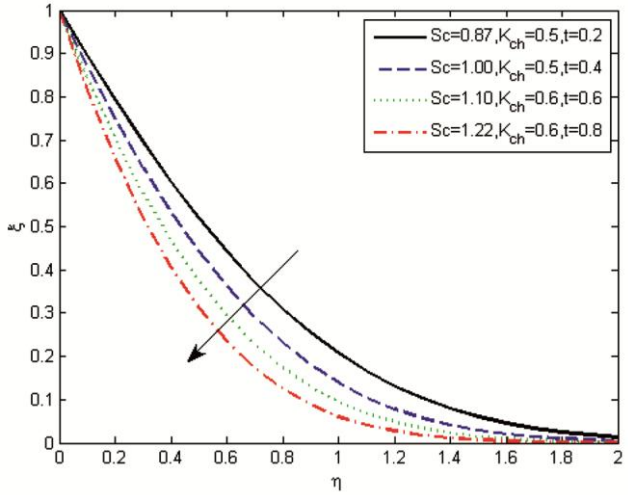

Fig. 11 — Concentration profiles for different Sc, K_{ch} and time t.

noticed in Figure 9 the temperature increases as the value of Ra and time t enhances. Physically, this means that as Ra improves, the amount of heat energy transfers to the fluid is improved. From Figure 10, we can observe that the temperature decreases for aluminum oxide-water nanofluid as the value of nanoparticle volume concentration ϕ and time t increases. From Figure 11, we can observe that the depiction of mass reduces for K_{ch}, Sc, and t value improves.

Conclusions

In the present work, we have studied an unsteady natural convective motion of a nanofluid over an infinite vertical sheet with the magnetic field, heat source and radiation effect. The dimensionless PDEs along with the limiting situations are explained by applying the Laplace transform method. The momentum, energy and concentration profiles of different types of nanofluid along with different nanoparticle volume concentrations are studied. The analytical and numerical results are also derived for the Nusselt number and skin friction coefficient.

In this paper we can summarize this analysis as follows:

It is proved that the momentum decreases as the value of nanoparticle volume concentration ϕ increases and the velocity reduce as the value of Hartmann number M enhances. The temperature decreases as the value of the heat generation parameter Q, Ra and time t increases. The temperature decreases for aluminum oxide-water nanofluid as the value of nanoparticle volume concentration φ and time t enhances. The Nusselt number reduces with an enhance in the nanoparticle volume concentration ϕ. The skin friction coefficient C_f enhances as nanoparticle volume concentration ϕ increases. It is also proved that as time increases, the skin friction coefficient decreases and becomes negative, which proves that a reverse type of flow arises near the plate.

Acknowledgments

The authors are grateful to Prof. G. C. Sharma, Agra University, Agra, India for his help and valuable suggestions to prepare this article and thanks to reviewers also.

Conflict of Interest

The authors declare that they have no conflict of interest.

Author Contributions

RPS and OP designed the model, computational framework and analyzed the data. RPS and PSR carried out the implementation. OP performed the calculations. RPS and OP wrote the manuscript with input from all authors. RPS and SRM conceived the study and were in charge of overall direction and planning.

References

1 Choi S U S, Enhancing thermal conductivity of fluids with nanoparticles, in developments and applications of non-Newtonian flows, *Amer Soc Mech Eng*, 231 (1995) 99-105.

2 Parida S K & Mishra S R, Heat and mass transfer of MHD stretched nanofluids in the presence of chemical reaction, *J Nanofluids*, 8 (1) (2019) 143-149.

3 Kuznetsov A V & Nield D A, Natural convective boundary-layer flow of a nanofluid past a vertical plate, *Int J Therm Sci*, 49 (2010) 243-247.

4 Wakif A, Boulahia Z, Mishra S R, Rashidi M M & Sehaqui R, Influence of a uniform transverse magnetic field on the thermo-hydrodynamic stability in water-based nanofluids with metallic nanoparticles using the generalized Buongiorno's mathematical model, *Eur Phys J Plus*, 133 (5) (2018) 1-16.

5 Makinde O D & Mishra S R, On stagnation point flow of variable viscosity nanofluids past a stretching surface with radiative heat, *Int J Appl Comput Math*, 3 (2) (2017) 561-578.

6 Sithole H M, Mondal S, Sibanda P & Motsa S S, An unsteady MHD Maxwell nanofluid flow with convective boundary conditions using spectral local linearization method, *Open Phys*, 15 (2017) 637-646.

7 Hayat T, Qayyum S, Alsaedi A & Shafiq A, Inclined magnetic field and heat source/sink aspects inflow of nanofluid with nonlinear thermal radiation, *Int J Heat Mass*

Tran, 103 (2016) 99-107.

8 Stokes G G, On the effects of an internal fraction of fluids on the motion of pendulums, *Cambridge Philos Trans*, 9 (1851) 8-106.

9 Raptis A A & Tzivanidis G J, Effects of mass transfer, free-convection currents and heat sources on the Stokes problem for an infinite vertical plate, *Astrophys Space Sci*, 78 (2) (1981) 351-357.

10 Masuda H, Ebata A, Teramae K & Hishinuma N, Alteration of thermal conductivity and viscosity of liquid by dispersing ultra-fine particles. Dispersion of $C-_{Al_2O_3,}$ SiO_2 and TiO_2 ultra-fine particles, *Netsu Bussei*, 7 (4) (1993) 227-233.

11 Lee S, Choi S U S, Li S & Eastman J A, Measuring thermal conductivity of fluids containing oxide nanoparticles, *J Heat Trans-T-ASME*, 121 (2) (1999) 280-289.

12 Xuan Y & Li Q, Heat transfer enhancement of nanofluids, *Int J Heat Fluid Flow*, 21 (2000) 58-64.

13 Xuan Y & Roetzel W, Conceptions for heat transfer correlation of nanofluids, *Int J Heat Mass Tran*, 43 (19) (2000) 3701-3707.

14 Pak B C & Cho Y I, Hydrodynamic and heat transfer study of dispersed fluids with submicron metallic oxide particles, *Exp Heat Tran*, 11 (2) (1998) 151-170.

15 Wen D & Ding Y, Natural Convective Heat Transfer of Suspensions of Titanium dioxide Nanoparticles (Nanofluids), *IEEE Trans Nanotechnol*, 5 (3) (2006), 220–227.

16 Loganathan P, Chand P N & Ganeshan P, Radiation effects on an unsteady natural convective flow of a nanofluid past an infinite vertical plate, *NANO*, 8 (1) (2013) 1350001-1350010.

17 Rohni A M, Ahmad S & Pop I, Flow and heat transfer over an unsteady shrinking sheet with suction in nanofluids, *Int J Heat Mass Tran*, 55 (2012) 1888-1895.

18 Bachok N, Ishak A & Pop I, The boundary layers of unsteady stagnation-point flow in a nanofluid, *Int J Heat Mass Tran*, 55 (2012) 6499-6505.

19 Sheikholeslami M, Ganji D D, Javed M Y & Ellahi R, Effect of thermal radiation on magnetohydrodynamics nanofluid flow and heat transfer employing two-phase model, *J Magn Magn Mater*, 374 (15) (2015) 36-43.

20 Sheikholeslami M & Ganji D D, Entropy generation of nanofluid in the presence of magnetic field using Lattice Boltzmann Method, *Physica A*, 417 (2015) 273-286.

21 Sheikholeslami M & Rashidi M M, Effect of space-dependent magnetic field on free convection of Fe3O4–water nanofluid, *J Taiwan Inst Chem E*, 56 (2015) 6-15.

22 Sheikholeslami M, Hayat T & Alsaedi A, MHD free convection of Al_2O_3–water nanofluid considering thermal radiation: A numerical study, *Int J Heat Mass Tran*, 96 (2016) 513-524.

23 Sheikholeslami M, Rashidi M M & Ganji D D, Effect of non-uniform magnetic field on forced convection heat transfer of Fe3O4-water nanofluid, *Comput Methods Appl Mech Eng*, 294 (2015) 299-312.

24 Khan W A & Pop I, Boundary-layer flow of a nanofluid past a stretching sheet, *Int J Heat Mass Tran*, 53 (2010) 2477-2483.

25 Das S, Jana R N & Chamkha A J, Unsteady free convection flow past a vertical plate with heat and mass fluxes in the presence of thermal radiation, *J Appl Fluid Mech*, 8 (4) (2015) 845-854.

26 Shehzad S A, Hayat T & Alsaed A, Influence of convective heat and mass conditions in MHD flow of nanofluid, *B Pol Acad Sci- Tech*, 63 (2) (2015) 465-474.

27 Hayat T, Imtiaz M, Alsaedi A & Kutbi M A, MHD three-dimensional flow of nanofluid with velocity slip and nonlinear thermal radiation, *J Magn Magn Mater*, 396 (2015) 31-47.

28 Das S, Jana R N & Makinde O D, Transient natural convection in a vertical channel filled with nanofluids in the presence of thermal radiation, *Alex Eng J*, 55 (2016), 253-262.

29 Kameswaran P K, Sutradhar A, Murthy P V S N & Sibanda P, Stagnation point flow and convection in a nanofluid saturated porous medium with convective boundary condition and chemical reaction, *J Nanofluids*, 5 (2016) 310-319.

30 Awad F G, Sibanda P & Murthy P V S N, A note on double dispersion effects in a nanofluid flow in a non-Darcy porous medium, *J Heat Trans*, 137 (2015) 1045011-1045015.

31 Rashadi A M, Chamkha A J, Reddy C R & Murthy P V S N, Effect of viscous dissipation on mixed convection in a nanofluid saturated non-Darcy porous medium under convective boundary condition, *J Nanofluids*, 4 (2015) 548-559.

32 Tiwari R K & Das M K, Heat transfer augments in a two-sided lid-driven differentially heated square cavity utilizing nanofluids, *Int J Heat Mass Tran*, 50 (9-10) (2007) 2002-2018.

33 Schlichting H & Gersten K, *Boundary Layer Theory*, (Spriger-Verlag, Berlin) 2001.

34 Brewster M Q, *Thermal radiative Transfer, and properties*, (John Wiley and Sons, New York, USA,) 1992.

35 Raptis A, Perdikis C & Takhar H S, Effect of thermal radiation on MHD flow, *Appl Math Comput*, 153 (2004) 645-649.

36 Mahmoud M M A, Thermal radiation effects on MHD flow of a micropolar fluid over a stretching surface with variable thermal conductivity, *Physica A*, 375 (2007) 401- 410.